

# A Model-Based Approach for Jet Aircraft Lateral Motion Control with Constraints Satisfaction

Zeeshan Rashid<sup>1\*</sup>, Shadi Khan Baloch<sup>2</sup>, Ghulam Amjad Hussain<sup>3</sup>

1. Department of Electrical Engineering, The Islamia University of Bahawalpur, Pakistan

2. Department of Electrical Engineering, Institute of Business Management (IoBM), Karachi Pakistan

3. Department of Electrical Engineering, College of Arts and Sciences, American University of Kuwait, Safat, Kuwait

\* **Corresponding Author:** Email: zeeshan.rashid@iub.edu.pk

## Abstract

*Design of a potentially robust autopilot to control lateral motion of a jet aircraft for maintaining the balance, turbulence rejection, handling asymmetric wind pressure, linearization and constraints on the inputs imposes technological and computational challenges for certain control algorithms. Especially, when the multiple states and inputs are strongly coupled to each other, it is imperative to evaluate the performance of most efficient control schemes which not only provide stable and error free response but also fulfill the system requirements with minimum computational cost. This paper demonstrates lateral motion control of a jet aircraft using state feedback controllers, proportional integral derivative controller and model predictive controller to evaluate and compare the control objectives. In a block diagram framework as a function of elementary tuning parameters, all strategies are implemented on a linearized state space model which is furnished by the set of fundamental equations of motion. The effects of disturbance, input and output constraints, sampling time and different controller gains are studied for the underlying multiple input multiple output system. State feedback algorithms provide minimum flexibility to achieve the control objectives in restraining the output within constraint boundaries. Proportional integral derivative controller is more flexible, yet not able to impose the limitation on both the input/output pair. Finally, model predictive controller presents the most efficient features by virtue of response time, robustness, stability, cost and constraints fulfillment with minimal computation and input cost.*

**Key Words:** Adaptive and feedback control, Aerodynamics, Aircraft, Computational effort, Computer modeling, Dynamic characteristics

## 1. Introduction

The reliability of flight control system of a jet aircraft, due to the technological developments has increased over time but the failure of the hydraulic control actuating system of the jet aircraft is still an open issue [1]. In such failures, the longitudinal motion (pitch) of aircraft can be controlled using collective throttle inputs, while its lateral motion is controlled by differential throttle inputs. Engine thrust of a crippled airplane in case of control surface failure may be used for back up control of airplane. Therefore, in order to handle such failures in emergency situations, the study of the lateral motion of an aircraft possesses paramount importance.

Different control schemes have been introduced in the literature for the lateral/longitudinal motion control of an aircraft. Conventional controller such as proportional integral derivative (PID) control for autopilot in micro air vehicles (MAVs) has been implemented by Chen et al. where a modified PID controller is used and coefficients of PID controller which can

discard disturbances and operate the MAV in stable positions have been derived [2]. Nair et al. studied aircraft yaw control system using linear quadratic regulator (LQR) and fuzzy logic controller (FLC) [3]. They have shown that the performance of LQR is better compared to a fuzzy design. The optimal control for the unmanned aerial vehicle (UAVs) control systems has been highlighted by Raffo et al. where LQR based design method using calculus of variations has been presented [4]. In another study, Giacomo et al. has studied the modeling and verification process for the stability and control of the aircraft and investigated the longitudinal and lateral/directional aerodynamic moments and effects [5]. Jonckheere et al. have introduced gain scheduling for lateral motion of propulsion controlled aircraft (PCA) using neural networks [1]. They have adopted PCA system for the emergency flight control of airplane in lateral motion and have used various  $H_\infty$  controllers at different conditions to train a radial base network (RBN) for gain scheduling. They have shown an improved performance for the control of different

dynamic relations in an aircraft. Lungu et al. demonstrated automatic control of aircraft lateral motion using neural networks and radio technical subsystems during landing [6]. They used a radio navigation system to calculate the distance between the aircraft and runway and an adaptive controller for the control of aircraft roll angle and its deviation from the runway. Lu et al. proposed adaptive differential thrust methodology for a commercial aircraft with damaged vertical stabilizer to regain its lateral stability [7]. They modeled the propulsion dynamics using differential equations to map the rudder input to differential thrust input and concluded that they were able to track the reference in extreme scenario in a stable way. Recently, Ahmed et al. addressed controller designs for lateral/longitudinal motion autopilots for F-16 aircraft using PID and LQR controllers after linearizing the nonlinear models around the equilibrium points [8]. By using careful tuning of the parameters in both feedback strategies, they performed comparative analysis of the set point tracking and evaluated the effectiveness of the controllers in MATLAB/SIMULINK environment.

Conventional controller such as PID is widely used due to the simplicity of its design and implementation. However, the design of PID is limited to single-input single-output (SISO) systems and cannot handle constraints, making it unsuited for many applications such as systems involving strongly coupled multi-input multi-output (MIMO) dynamics. Common dynamic characteristics that are difficult for PID controllers include large time delays and higher order dynamics. Model-based techniques such as pole assignment by state feedback [9, 10], LQR method [11, 12] and linear quadratic Gaussian with loop transfer recovery (LQG/LTR) [13] are widely used in control system and are able to handle MIMO systems. The models used in such control techniques represent the behavior of underlying (potentially) complex dynamical systems and are used to predict the system behavior in response to measured inputs and unmeasured disturbances; the main drawback being their inability to handle constraints.

One of main advantages of using model predictive control (MPC), compared to other model-based approaches, is its ability to handle constraints, e.g. constraints defined on inputs, outputs or states. MPC uses a feedback strategy such that it determines (estimates) the current state of the system, optimizes the control objective (e.g. tracking) for a finite horizon and apply the first set of optimized control strategy. MPC determines the

ongoing plant output, dynamic state of the process, the system models, the set points and limits to calculate future changes in the dependent variables as shown in Fig. 1. The objective of these optimizations is to grip the dependent variables close to the target while maintaining the constraints on both independent and dependent variables. MPC customarily implements the first change in each independent variable, and reiterates the computation until the next change is essentially required. Owing to its appealing features, there has been considerable recent work in the field of aerodynamics including MPC for unmanned aerial vehicles to control quad rotor platform [14] and for glide slope tracking during landing [15]. However, there exists an extremely limited research work in the open literature dealing with MPC implementation for lateral motion control of jet aircraft.

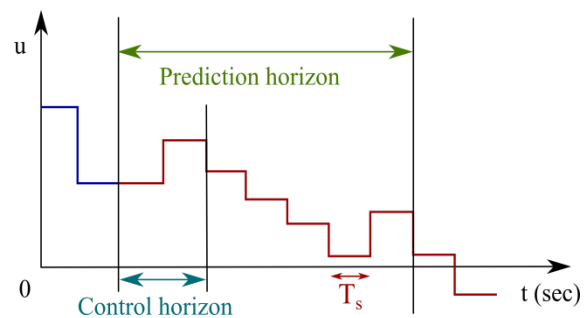


**Fig. 1:** Model-predictive control (MPC) receding horizon principle

This work is aimed at controlling yaw rate and the bank angle for the lateral motion of a jet aircraft in response to rudder deflection and aileron deflection. In such a control problem, constraints on the states, outputs and specially inputs are very critical. Though, the dynamics of a jet aircraft are typically nonlinear in nature, a linearized model is considered at a certain altitude for the design of MPC controller. For the sake of comparison, conventional PID controller is also designed with linearized dynamics. Model-based designs such as LQR and pole placement are also used, where it is shown to have satisfactory performance at the cost of constraints violation. At the end, robustness of the MPC design is tested compared to LQR design.

The paper is organized as follows: In section 2, the linearized dynamic model of jet aircraft has been presented and the controllability and observability of the system are determined. In section 3, different control schemes such as state feedback, PID and MPC are applied to the problem and the main results are analyzed under different tuning conditions. Conclusions are finally drawn in section 4.

## 2. Dynamic Model of Jet Aircraft

Sky view of the jet aircraft along with the axis of rotation is labeled in Fig. 2. The lateral motion deals with the rotation of the jet aircraft in the azimuth plane. There are two parts of the aircraft which are responsible for the lateral motion, rudder which rotates it about the yaw axis and ailerons which rotate it about the roll axis. When left side of the aileron is made to push down and the right side to up, this will cause the aircraft to be up from the left side and down from the right side. The rudder is also made to rotate towards right. This orientation of the input states will cause the plane to rotate towards right side and vice versa.

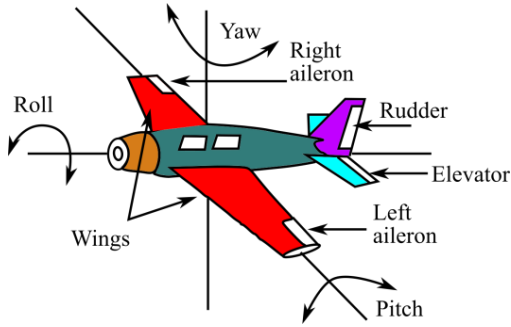


**Fig. 2:** Sky view of jet aircraft

Fundamentally, there are six equations of motion consisting of three equations (along 3D axis) for each longitudinal and lateral direction. The equations of motion along the lateral direction are shown below [16].

$$y = m[\dot{\beta} + U_0 r - W_0 \varepsilon - g \cos \theta_0 \Phi] \quad (1)$$

$$n = I_{zz} \dot{r} - I_{xz} \dot{\varepsilon} \quad (2)$$

$$l = I_{xx} \dot{\varepsilon} - I_{xz} \dot{r} \quad (3)$$

$$\varepsilon = \dot{\Phi} - \psi \sin \theta_0 \quad (4)$$

$$r = \psi \cos \theta_0 \quad (5)$$

Here  $\psi$  is the rate of turn and  $I_{xx}$  (and  $I_{zz}$ ) and  $I_{xz}$  are called moment of inertia and product of inertia respectively. Note that Eqs. (2) and (3) contain two derivative terms each making it impossible to represent them in state space due to nonlinearity. Expanding the left hand sides of equations, (1) – (5) using Taylor's series ( $\frac{\partial y}{\partial \beta} \beta + \frac{\partial y}{\partial r} r + \dots$ ) with respect to  $\beta$ ,  $r$ ,  $\varepsilon$  and

their derivatives along with the inputs, following expressions of linear system are obtained.

$$\dot{\beta} = Y_{\beta} \beta - U_0 r + W_0 \varepsilon + g \cos \theta_0 \Phi + Y_{\delta_R} \delta_R \quad (6)$$

$$\dot{r} = N_{\beta} \beta + N_r r + N_{\varepsilon} \varepsilon + N_{\delta_R} \delta_R + N_{\delta_A} \delta_A \quad (7)$$

$$\dot{\varepsilon} = L_{\beta} \beta + L_r r + L_{\varepsilon} \varepsilon + L_{\delta_R} \delta_R + L_{\delta_A} \delta_A \quad (8)$$

$$\dot{\Phi} = r \tan \theta_0 + \varepsilon \quad (9)$$

The system has two inputs: Rudder deflection ( $\delta_R$ ) and aileron deflection ( $\delta_A$ ). The system has four states namely, sideslip ( $\beta$ ), yaw rate ( $r$ ), roll rate ( $\varepsilon$ ) and bank angle ( $\Phi$ ) with  $r$  and  $\Phi$  being the two outputs.  $Y_{\beta}$ ,  $Y_{\delta_R}$  are termed as side slip derivative and rudder deflection derivative respectively.  $N_{\beta}$ ,  $N_r$ ,  $N_{\varepsilon}$ ,  $N_{\delta_R}$  and  $N_{\delta_A}$  are termed as yawing moments along sideslip, yaw axis, roll axis rudder deflection and aileron deflection respectively.  $L_{\beta}$ ,  $L_r$ ,  $L_{\varepsilon}$ ,  $L_{\delta_R}$  and  $L_{\delta_A}$  are termed as rolling moments along sideslip, yaw axis, roll axis rudder deflection and aileron deflection respectively.  $U_0$  and  $W_0$  are the translational velocity components along  $x$ - and  $z$ -axis respectively when the aircraft is in stationary condition.  $g$  is the acceleration due to gravity and  $\theta_0$  is the angle of gravity vector with body axis system. The mathematical expressions and numerical values of all variables involved in the state space model are elaborated in [17]. An airplane undergoes both yawing moment and bank angle change in response to each of the inputs which implies that the inputs and outputs are strongly coupled to each other. In addition, yawing moment due to  $\delta_R$  also causes the aircraft to undergo rolling moment, that's why; the states are also coupled to each other. The dynamic model derivation of jet aircraft starts from the Newton's second law of motion. Initially, the body axis of the system is converted to the earth axis taking into account angular momentum, torque and inertia followed by the inclusion of gravity effects [18]. Equations of lateral motion are derived at equilibrium which are coupled and nonlinear in nature. The next task is to linearize the model at the steady state by making the Jacobian matrix of the system and put the states at the equilibrium point which is the reference  $\gamma$ .

$$x = \begin{bmatrix} \beta \\ r \\ \varepsilon \\ \Phi \end{bmatrix}, \quad u = \begin{bmatrix} \delta_R \\ \delta_A \end{bmatrix}, \quad y = \begin{bmatrix} r \\ \Phi \end{bmatrix}$$

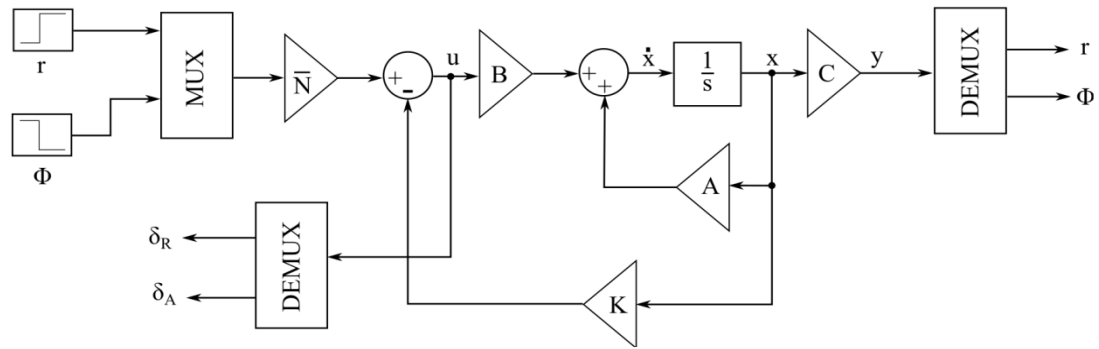


**Fig. 3:** Block diagram of state feedback control

The resulting state space model is shown in Eq. (10) where the parameter values in the  $A$  and  $B$  matrices were calculated by Chvojka [19]. The control system under consideration is applied on the linearized model of lateral motion during a cruise flight at a speed of  $MACH = 0.8$  and height of  $40,000$  ft [20]. The system is both controllable and observable as is given by the positive definite solution of Lyapunov equations yielding corresponding Gramian matrices [21]. Due to physical limitations, inputs and outputs of the system are constrained below certain level. For a safe operation,  $\delta_R$  and  $\delta_A$  are constrained under  $80^\circ$  and  $35^\circ$  respectively. The system overshoot ( $OS$ ) of  $r$  should be less than  $15^\circ/sec$  and  $OS$  of  $\Phi$  should be within  $9^\circ$ . The settling time ( $t_s$ ) of the system should not be more than  $7.5$  sec. Step reference is  $\gamma = [2, -2]$ .

$$\dot{x} = Ax + Bu \quad (10a)$$

$$y = Cx + Du \quad (10b)$$

$$A = \begin{bmatrix} -0.0558 & -0.9968 & 0.0802 & 0.0415 \\ 0.5980 & -0.1150 & -0.0318 & 0 \\ -3.0500 & 0.3880 & -0.4650 & 0 \\ 0 & 0.0805 & 1 & 0 \end{bmatrix}$$

$$B = \begin{bmatrix} 0.0073 & 0 \\ -0.4750 & 0.0077 \\ 0.1530 & 0.1430 \\ 0 & 0 \end{bmatrix}$$

$$C = \begin{bmatrix} 0 & 1 & 0 & 0 \\ 0 & 0 & 0 & 1 \end{bmatrix} D = \begin{bmatrix} 0 & 0 \\ 0 & 0 \end{bmatrix}$$

$$x_0 = [1 \quad 1 \quad 1 \quad 0]^T$$

### 3. Control Schemes for Lateral Motion Dynamics

In this section, implementation of three main types of control systems namely, state feedback control, PID control and MPC system are demonstrated. The aim is to satisfy the constraints and automatize the coupled system in a stable and error-free manner which is a challenging task.

### 3.1 State Feedback Control Method

In this subsection, model-based approach for controlling the lateral motion dynamics, specifically by using LQR and pole-placement method is designed. Figure 3 shows the block diagram of the closed loop system incorporating the feedback gain matrix,  $K$ , and all system matrices. The outputs are fed back where they are compared to the corresponding references to generate the error signal which is the input. All inputs and outputs can be viewed by the use of separate scopes for the analysis.

#### 3.1.1 LQR Method

In optimal control problems, one of the main concerns is to regulate the system output minimizing the cost function,  $J$ , which is defined as the sum of deviations of control parameters from their reference values.  $J$  is minimized by optimizing  $K$  which is further a function of symmetric positive constant matrix  $P$ .  $P$  matrix can be calculated by solving continuous time algebraic Riccati equation iteratively due to its transcendental nature [22]. Assuming infinite horizon control design, all the functions and matrix variables are mathematically expressed in Eq. (11).

$$J = \int_0^\infty (x^T Q x + u^T R u) dt \quad (11a)$$

$$u = -kx \quad (11b)$$

$$K = R^{-1} B^T P \quad (11c)$$

$$A^T P + PA - PBR^{-1}B^T P + Q = 0 \quad (11d)$$

$Q$  and  $R$  are the diagonal matrices whose entries,  $q_i$  and  $r_i$  respectively for the  $i^{th}$  state are evaluated according to the system requirements.  $q_i = \frac{1}{t_{s,i} x_{i,max}^2}$ , where  $t_{s,i}$  and  $x_{i,max}$  are the settling time and peak  $OS.R = \rho [r_j]_{diag}$ , where  $r_j = \frac{1}{u_{j,max}^2}$ , and  $u_{j,max}$  is the maximum constraint on the  $j^{th}$  input and  $\rho$  is chosen to trade-off between

regulation and control effort. The resultant  $Q$  and  $R$  are adjusted to  $\begin{bmatrix} 0 & \frac{1}{7.5 \times (15)^2} & 0 & \frac{1}{7.5 \times (9)^2} \end{bmatrix}_{diag}$  and  $\rho = \begin{bmatrix} \frac{1}{80^2} & \frac{1}{35^2} \end{bmatrix}_{diag}$  respectively for  $\rho$  of 0.1 and 1 to quantify  $K$ . The closed loop system is unable to stabilize at the desired reference which necessitates pre-compensation using feedforward gain matrix,  $\bar{N}$ , as shown in Fig. 3.  $\bar{N}$  matrix can be calculated assuming the steady state condition ( $s = 0$ ) in the transfer function matrix,  $G(s)$ , after equating it to 1 [ $G(0) = 1$ ] as represented in Eq. (12).

$$G(s) = \frac{Y(s)}{R(s)} = C(SI - A)^{-1}B\bar{N} \quad (12a)$$

$$\bar{N} = [-C(A - BK)^{-1}B]^{-1} \quad (12b)$$

The resultant output response of jet aircraft is plotted in Fig. 4 which clearly shows that the system is not only stable but also settling to the desired reference. For a value of  $\rho$  equal to 0.1,  $OS$  is calculated to be  $43.12^\circ$  and  $21.18^\circ$  for the two outputs, corresponding  $t_s$  are 4.23 sec, 3.20 sec and maximum swing in the inputs are calculated to be  $471^\circ$  and  $88^\circ$ .

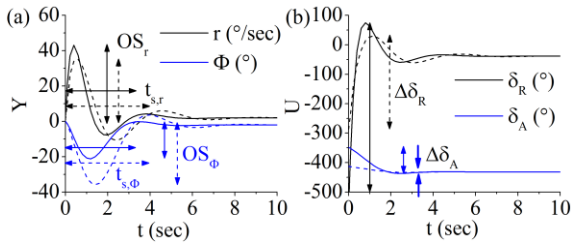


**Fig. 4:** (a) Output and (b) input response by LQR control method with  $\rho = 0.1$  (-----) [ $OS_r = 41.12^\circ/\text{sec}$ ,  $OS_\phi = 19.18^\circ$ ,  $t_{sr} = 4.23$  sec,  $t_{s,\phi} = 3.20$  sec,  $\Delta\delta_R = 471^\circ$ ,  $\Delta\delta_A = 88^\circ$ ] and  $\rho = 1$  (- - -) [ $OS_r = 35.10^\circ/\text{sec}$ ,  $OS_\phi = 35.84^\circ$ ,  $t_{sr} = 4.00$  sec,  $t_{s,\phi} = 3.90$  sec,  $\Delta\delta_R = 317^\circ$ ,  $\Delta\delta_A = 20.20^\circ$ ]

When the value of  $\rho$  is increased to 1,  $OS$  is calculated to be  $35.10^\circ$  and  $35.84^\circ$  for the two outputs, corresponding  $t_s$  are 4.00 sec, 3.90 sec and maximum swing in the inputs are calculated to be  $317^\circ$  and  $20.20^\circ$ . Clearly, most of the values exceed the requirements of the system which imposes a technical limitation on the implementation of this control scheme for lateral motion.

### 3.1.2 Pole Placement Method

Pole placement method is another powerful technique employed to assign the closed loop poles of a system at predetermined locations in the  $s$ -plane. In this way, not only the instability can be

resolved, but also system dynamics can be precisely tuned according to the constraints. There are four poles of the open loop system which lie at  $-0.0073$ ,  $-0.5627$  and  $-0.0329 \pm 0.947i$ . Before designing a controller using pole placement technique, it is notable that the closed loop poles should not be far away from the open loop poles of the system otherwise; the system will demand high control effort. Secondly, the closed loop poles should not be very negative otherwise; the system will be fast reacting with high bandwidth amplifying the noise significantly. The resultant  $K$  matrix can be calculated by using Ackermann's formula.

Figure 5 shows the output and input response of jet aircraft assuming the closed loop poles located at  $[-0.8 -0.9 -1 -3]$  (solid lines). For a value of first assigned pole,  $s_1$ , equal to  $-0.8$ ,  $OS$  is calculated to be  $11.97^\circ/\text{sec}$  and  $2.15^\circ$  for the two outputs, corresponding  $t_s$  are 2.98 sec, 2.58 sec and maximum swing in the inputs are calculated to be  $66.08^\circ$  and  $398.25^\circ$ . When the closed loop poles are placed at  $[-1.8 -0.9 -1 -3]$  (dashed lines), the system oscillations are reduced and it stabilizes to the set point in a shorter time.

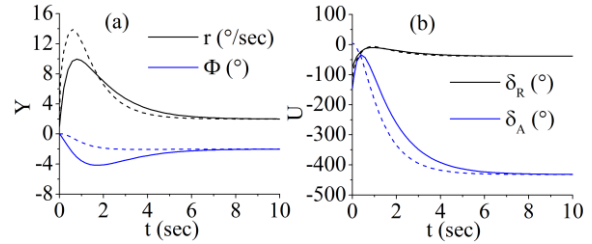


**Fig. 5:** (a) Output and (b) input response by pole placement method with  $s_1 = -0.8$  (-----) [ $OS_r = 11.97^\circ/\text{sec}$ ,  $OS_\phi = 2.15^\circ$ ,  $t_{sr} = 2.98$  sec,  $t_{s,\phi} = 2.58$  sec,  $\Delta\delta_R = 66.08^\circ$ ,  $\Delta\delta_A = 398.25^\circ$ ] and  $s_1 = -1.8$  (- - -) [ $OS_r = 11.97^\circ/\text{sec}$ ,  $OS_\phi = 0^\circ$ ,  $t_{sr} = 3.78$  sec,  $t_{s,\phi} = 1.18$  sec,  $\Delta\delta_R = 125.56^\circ$ ,  $\Delta\delta_A = 436.12^\circ$ ]

In this case,  $OS$  is calculated to be  $11.97^\circ/\text{sec}$  and  $0^\circ$  for the two outputs, corresponding  $t_s$  are 3.78 sec, 1.18 sec and maximum swing in the inputs are calculated to be  $125.56^\circ$  and  $436.12^\circ$ . The system undergoes some oscillations before settling to the reference values and there is also some  $OS$  in the system. However, as expected, the cost of the control action is increased and there is slightly higher value of  $\Delta\delta_A$  as shown in Fig. 5(b). As observed, above mentioned control schemes are failed to keep the inputs under constraints with both types of state feedback control methods.

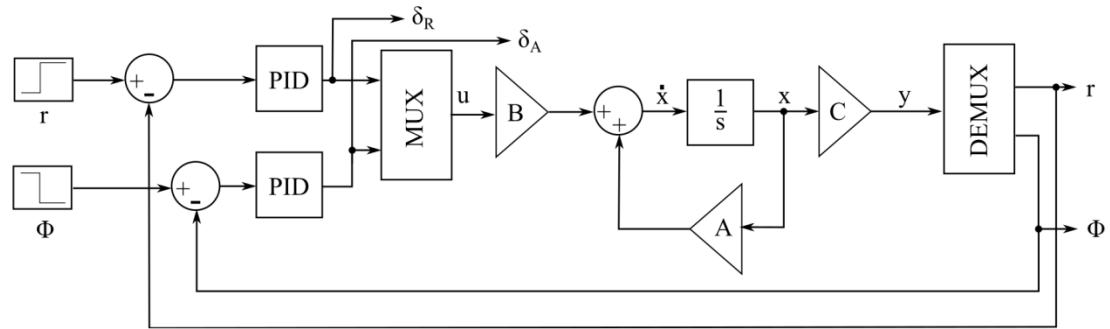


Fig. 6: PID control without decoupling of the system

### 3.2 PID Control Method

#### 3.2.1 Coupled System

This section deals with the implementation of PID control over the MIMO system which is a popular method to meet the design requirements. When the system is not decoupled as shown in Fig. 6, it takes forever to stabilize to the set point value since all the states are mutually dependent on each other.

The output and input responses of the coupled system are plotted in Fig. 7 after some parametric tuning which clearly shows that  $\Phi$  stabilizes after  $3 \times 10^5$  sec and the input constraints are also beyond the allowable limits.

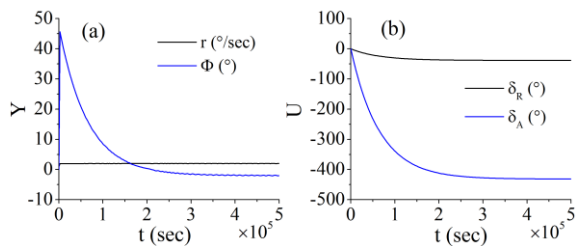


Fig. 7: (a) Output and (b) input response by coupled PID control.  $OS_r = 1^\circ/\text{sec}$ ,  $OS_\Phi = 47^\circ$ ,  $t_{s,r} = 2246$  sec,  $t_{s,\Phi} = 1.5 \times 10^5$  sec,  $\Delta\delta_R = 38.4^\circ$ ,  $\Delta\delta_A = 431^\circ$

#### 3.2.2 Decoupled System

A more efficient control scheme is implemented in Fig. 8 incorporating a negative feedback inner loop containing the decoupling matrix, T. Signal outputs from the decoupling matrix are compared with the corresponding control signals before being fed to the aircraft system. The input of the PID controller is the comparator signal from the reference commands and the actual output without any gain block. Such a two level feedback system provides a robust and isolated control of the system providing exact agreement with the output constraints.  $OS$  in the two outputs are calculated to be  $0.18^\circ/\text{sec}$  and  $0.08^\circ$ ,  $t_s$  is found to be 0.06 sec and 0.03 sec and swings in the manipulated variables are  $3.39^\circ$  and  $6994^\circ$ . Clearly, the manipulated variable,  $\Delta\delta_A$ , is unbounded contradicting the constraints with this algorithm as well because additional blocks for controlling the system output have caused more controlling cost of the system resulting in a huge swing in the system input. The tuned parameters of the PID controller for coupled and decoupled systems are summarized in Table 1.

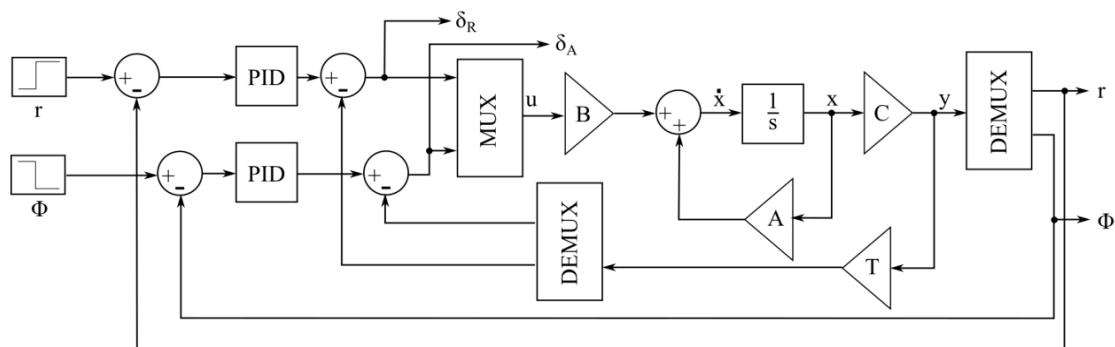
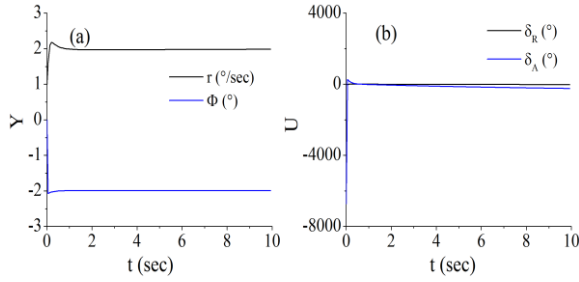


Fig. 8: PID control after decoupling of the system



**Fig. 9:** (a) Output and (b) input response by decoupled PID control.  $OS_r = 0.18^\circ/\text{sec}$ ,  $OS_\phi = 0.08^\circ$ ,  $t_{s,r} = 0.06 \text{ sec}$ ,  $t_{s;\phi} = 0.03 \text{ sec}$ ,  $\Delta\delta_R = 3.39^\circ$ ,  $\Delta\delta_A = 6994^\circ$

**Table 1:** Tuned parameters of PID controller

Block	$K_P$	$K_I$	$K_D$
PID <sub>r,c</sub>	0	-0.01	0
PID <sub>ϕ,c</sub>	0	0.0001	0
PID <sub>r,d</sub>	-42.56	-82.51	0.02
PID <sub>ϕ,d</sub>	4173.49	4167.40	-7.12

### 3.3 MPC Method

In this subsection, model predictive control of the aircraft is demonstrated under different configurations aimed for achieving the input and output requirements. Comprehensive block diagram of the closed loop system is shown in Fig. 10. Initially, the controller is assumed to have unbounded constraints and unweighted inputs. Weights for both outputs are considered to be 1, controller gain of 0.8, estimator gain of 0.5 and prediction/control horizons of 10/2 are assumed respectively.

#### 3.3.1 Effect of Control Interval

Figure 11 shows input and output responses of the system for a control interval of 0.01 [(a) and (b)] and 0.05 [(c) and (d)]. It can be observed that the system is unstable especially input,  $\delta_R$ , and

output,  $\Phi$ , are exploding at a massive rate.

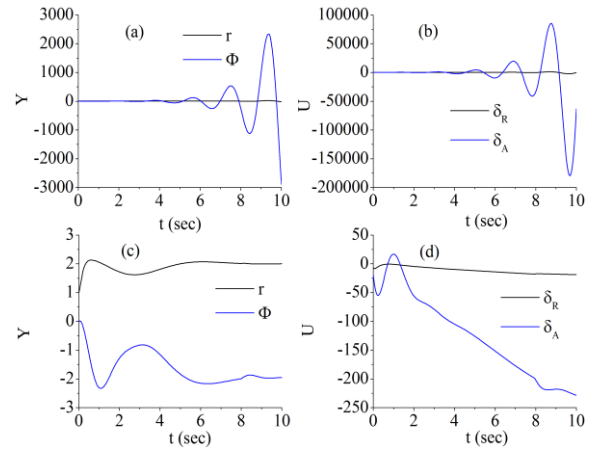


**Fig. 11:** (a) Output and (b) input response for a control interval of 0.01 sec. (a) Output and (b) input response for a control interval of 0.05 sec

However, when the control interval is increased five times, i.e. to 0.05, the system becomes stable with both the outputs stabilizing to the set points. This is due to the reason that MPC will predict less information from future time at smaller control interval and will take the control decision corresponding to the smaller future duration due to less control horizon.

#### 3.3.2 Effect of Prediction / Control Horizons

Figure 12 shows the input and output response of the system under an increased prediction and control horizon samples of 50 and 10 respectively. For more prediction and control horizons the response time becomes larger and the system takes longer to settle down to the set point references. As a result,  $OS$  in both the outputs reduces.

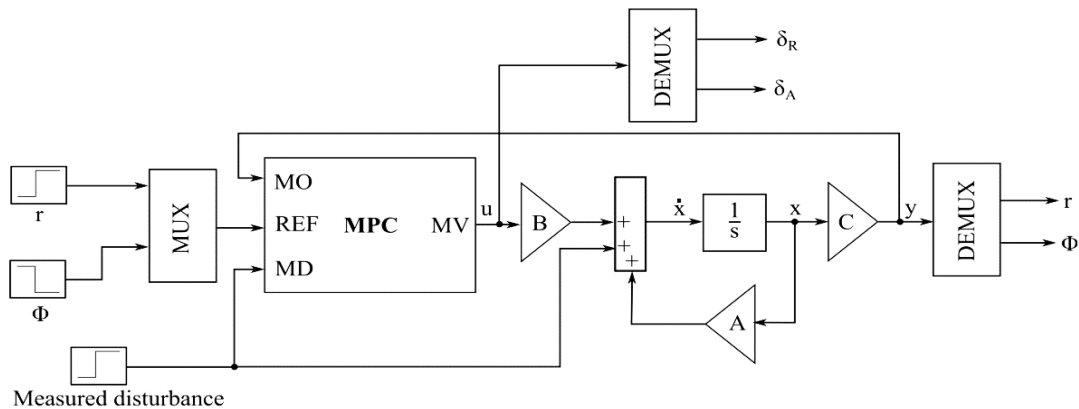


**Fig. 10:** Block diagram of MPC

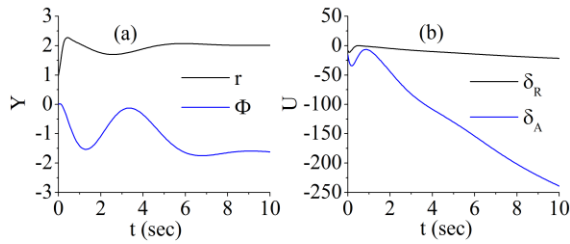


Fig. 12: (a) Output and (b) input response for Prediction/Control horizon of 25/10

### 3.3.3 Effect of Measured Disturbance

Considering the original horizon samples and control interval, the output is investigated by adding the constant measured disturbance of 2 as shown in Fig. 10. Interestingly, the system is able to stabilize at the set point. The input and output responses of the system are shown in Fig. 13.

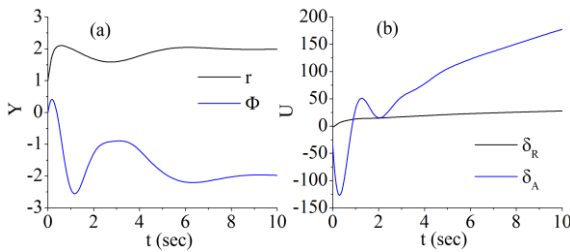


Fig. 13: (a) Output and (b) input response for a constant measured disturbance of 2

### 3.3.4 Robustness Test

The design of the controller is analyzed to check the robustness of the system. This is done by changing each entry of the state matrix by a certain percentage and check the system output if it is settling to the reference in a stable way. For this purpose, entries of matrix  $A$  are decided to increase by 10%, 30% and 50%. Figure 14 shows the input and output responses of the system after applying robustness test and clearly, the system is stable with minimum steady state error.

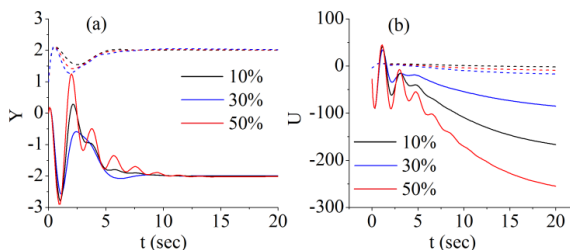


Fig. 14: (a) Output [ $r$  (dash),  $\Phi$  (solid)] and (b) input [ $\delta_R$  (dash),  $\delta_A$  (solid)] response for a slight variation in state matrix

### 3.3.5 Applying Constraints

So far, no constraints are applied to all the inputs/outputs of the system; yet, both outputs of the system are satisfying the constraints of  $OS$  and  $t_s$ . However, the inputs are unbounded and required constraints must be applied to bring them within allowable limits. Figure 15 shows the output and input responses of the algorithm after applying input and output constraints.  $OS$  in the two outputs are calculated to be  $0.15^\circ/\text{sec}$  and  $0.19^\circ$ ,  $t_s$  is found to be 3.95 sec and 5.00 sec and swings in the manipulated variables are  $9.60^\circ$  and  $35^\circ$ . Clearly, all the requirements of the system regarding  $OS$  and  $t_s$  are satisfied.

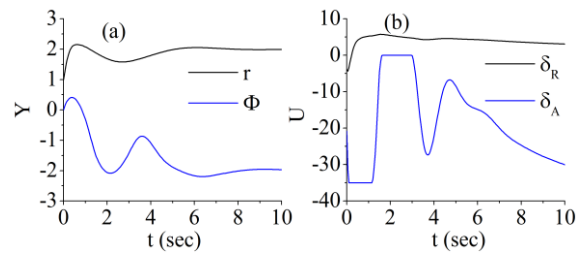


Fig. 15: (a) Output and (b) input response after applying the constraints.  $OS_r = 0.15^\circ/\text{sec}$ ,  $OS_\phi = 0.19^\circ$ ,  $t_{s,r} = 3.95$  sec,  $t_{s,\phi} = 5.00$  sec,  $\Delta\delta_R = 9.60^\circ, \Delta\delta_A = 35^\circ$

The overall results of the investigated control schemes are summarized in Table 2. It is notable that each method contains two sets of analysis apart from MPC method which contains only the final result after optimization. In the last row, the required response of input/output is provided which implies that only MPC method makes possible to achieve the desired target of the system.

Table 2: Summary of output and input response using different control methods

Type	$OS_r$ ( $^\circ/\text{sec}$ )	$OS_\phi$ ( $^\circ/\text{sec}$ )	$t_{s,r}$ (sec)	$t_{s,\phi}$ (sec)	$\Delta\delta_R$ ( $^\circ$ )	$\Delta\delta_A$ ( $^\circ$ )
LQR	41.12	19.18	4.23	3.20	471	88
	35.10	35.84	4.00	3.90	317	20.2
Pole Place	11.97	2.15	2.98	2.58	66.1	398
	11.97	0	3.78	1.18	126	436
PID	1	47	2246	$1.5 \times 10^5$	38.4	431
	0.18	0.08	0.06	0.03	3.39	6994
MPC	0.15	0.19	3.95	5.00	9.60	35
Reqd.	15	9	7.5	7.5	80	35

## 4. Conclusion

This paper presents implementation of control systems to stabilize the lateral motion of jet

aircraft during a cruise flight. Three popular types of control schemes namely (i) state feedback control, (ii) PID control and (iii) MPC have been implemented after fine tuning of the subsequent handling parameters. State feedback control is implemented using two methods (i) LQR and (ii) pole placement with the use of pre-compensation to remove steady state error and both of them yielded unconstrained  $OS$  and  $\Delta\delta$ . With PID control methodology, two schemes are considered namely (a) coupled and (b) decoupled. For coupled system, the outputs take almost infinite duration to stabilize and, in addition, almost all of the constraints are not satisfied even though the system ultimately meets the target. After decoupling, constraints over  $t_s$  and  $OS$  for both outputs are satisfied, whereas,  $\Delta\delta_A$  is found to be around  $7000^\circ$  due to increased cost of the control action. Finally, MPC method is applied to the system aiming at determining the response to meet the system requirements. Although, the outputs are found to be slowly stabilizing after some sluggish oscillations, however, both output and input transients stay within the allowable limits. The system response is investigated after applying disturbances and robustness tests have also been conducted with MPC, the results in all the cases are found promising. The final values of the model which yielded the best output response are summarized in Table 3.

**Table 3:** Tuned parameters of MPC

Control interval	0.05
Prediction horizon	10.00
Control horizon	2.00
Controller gain	0.80
Estimator gain	0.50
Input weights	0.00

Based on the above analysis, it is strongly concluded that applying MPC over MIMO system of jet aircraft has dominantly best features among all types of controllers. For a human controlled aircraft, inherent instability can be tolerated up to a certain level which a pilot can control; however, there is absolutely no margin for error when the aircraft is under the control of autopilot. In this regard, the aircraft should be able to stabilize itself in response to atmospheric turbulence, wind gradients and commands that come from navigation system during the lateral motion [23]. As a result, MPC possesses the most preferable choice to design autopilot for aircraft systems whose dynamics are strongly coupled and a minute disturbance in one state can cause severe

imbalance. This will result in fatal injury of a passenger, aircraft structural failure, aircraft disappearance or complete inaccessibility and significant eradication of urban infrastructure. MPC is also finding applications especially in chemical industry where constraint handling using a model-based approach is a critical issue [24, 25].

## 5. References

- [1] Jonckheere E. A., Yu G. R., and Chien. C. C., “Gain scheduling for lateral motion of propulsion controlled aircraft using neural networks”, Proceedings of the American Control Conference, Vol. 5, pp. 3321–3325, USA, 1997.
- [2] Chen X. H., Haq E. and Lin. J., “Design, modeling and tuning of modified PID controller for autopilot in MAVs”, IEEE/ACIS International Conference on Software Engineering, Artificial Intelligence, Networking and Parallel/Distributed Computing, pp. 475–480, China, 2016.
- [3] N.V.G., D.M.V. and George V., “Aircraft yaw control system using LQR and fuzzy logic controller”, International Journal of Computer Applications, Vol. 45, No. 9, pp. 25–30, 2012.
- [4] Raffo G.V., Ortega M. G. and Rubio F.R., “Back stepping/nonlinear  $H_\infty$  control for path tracking of a quad rotor unmanned aerial vehicle” , American Control Conference, pp. 3356-3361, USA, 2008.
- [5] Giacomo C., “Modeling, simulation and flight test for automatic flight control of the condor hybrid-electric remote piloted aircraft”, Ph.D. diss., Air Force Institute of Technology, USA, 2012.
- [6] Lungu M., and Lungu R., “Automatic control of aircraft lateral-directional motion during landing using neural networks and radio-technical subsystems”, Neurocomputing, Vol. 171, pp. 471–481, 2016.
- [7] Lu L. K. and Turkoglu K., “Adaptive differential thrust methodology for lateral/directional stability of aircraft with a completely damaged vertical stabilizer”, International Journal of Aerospace Engineering, Vol. 2018, pp. 1 – 19, 2018.
- [8] Ahmed W., Li Z., Maqsood H. and Anwar B., “System modeling and controller design

- for lateral and longitudinal motion of F-16”, *Automation Control and Intelligent Systems*, Vol. 4, No. 1, pp. 39 – 45, 2019.
- [9] Kautsky J., Nichols N.K. and Dooren P.V., “Robust pole assignment in linear state feedback”, *International Journal of Control*, Vol. 41, No. 05, pp. 1129 – 1155, 1985.
- [10] Wonham W. M., “On pole assignment in multi-input controllable linear systems”, *IEEE Transactions on Automatic Control*, Vol. 12, No. 06, pp. 660 – 665, 1967.
- [11] Broussard J. R., “A quadratic weight selection algorithm”, *IEEE Transactions on Automatic Control*, Vol. 27, No. 04, pp. 945 – 947, 1982.
- [12] D. Ali, L. Hend, and M. Hassani, “Optimized eigen structure assignment by ant system and LQR approaches”, *International Journal of Computer Science and Applications*, Vol. 5, No. 04, pp. 45 – 56, 2008.
- [13] Raemaekers A. J. M., “Design of a model predictive controller to control UAVs”, *Technische Universiteit Eindhoven*, Vol. 2007.141, 2007.
- [14] Ru P. and Subbarao K., “Non linear model predictive control for unmanned aerial vehicles”, Vol. 4, No. 31, pp. 1 – 26, 2017.
- [15] Misra G., and Bai X., “Output feedback stochastic model predictive control for glideslope tracking during aircraft carrier landing”, *Journal of Guidance, Control and Dynamics*, Vol. 42, No. 9, pp. 2098 – 2105, 2019.
- [16] McLean D., “Automatic flight control systems”, Prentice Hall International, 1990.
- [17] Lin P. N. W., Kham N. L. and Tun H. M., “Longitudinal and lateral dynamic system modeling of a fixed wing UAV”, *International Journal of Scientific and Technology Research*, Vol. 6, No. 4, pp. 171 – 174, 2017.
- [18] McClean D, “Automatic flight control systems”, Prentice Hall International Series in Systems and Control Engineering, 1990.
- [19] Chvojka M., “Dynamic characteristics of an airplane”, 2004.
- [20] Barsaiyan P. and Purwar S., “Comparison of state feedback controller design methods for MIMO systems”, *International Conference on Power, Control and Embedded Systems*, pp. 1 – 6, India. 2013.
- [21] Raczynski D, Stanisławski W., “Controllability and observability gramians parallel computation using GPU”, *Journal of Theoretical and Applied Computer Science*, Vol. 6, No. 01, pp. 47 – 66, 2012.
- [22] Purnawan H., Mardijah and Purwanto E. B., “Design of linear quadratic regulator (lqr) control system for flight stability of LSU-05”, *Journal of Physics: Conference Series*, Vol. 890, No. 01, pp. 012056, 2017.
- [23] Etkin B., Reid L. D., “Dynamics of flight: stability and control”, John Wiley & Sons, Inc., 3rd ed., 1959.
- [24] Rawlings J. B. and David M., “Model predictive control: theory and design”, Nob Hill Publishing, 2009.
- [25] Maciejowski J. M., “Predictive control: with constraints”, Pearson Education, 2002.